

Design Optimization of a Solar Air Collector Integrating a Phase Change Material

Martin Zálešák ^{a,*}, Lubomír Klimeš ^b, Pavel Charvát ^a

^aDepartment of Thermodynamics and Environmental Engineering, Brno University of Technology, Technická 2896/2, 61669 Brno, Czech Republic

^bSustainable Process Integration Laboratory—SPIL, NETME Centre, Brno University of Technology, Technická 2896/2, 61669 Brno, Czech Republic
162098@vutbr.cz

Solar radiation is a clean and renewable source of energy, which can be employed in various forms. In contrast to electricity, the use of solar energy in the form of heat is simple and straightforward. Solar air collectors (SAC), which convert solar radiation into heat and transfer it to the air, represent a way how to use solar energy for space heating in buildings. In the paper, the operation and optimal design of a solar air collector integrating a phase change material (PCM) for thermal energy storage is computationally investigated. A computer model of a front and back pass solar air collector with a PCM-based absorber was developed and validated against experimental data. The energy balance approach coupled with the control volume method was implemented for solving conduction heat transfer inside the PCM, and the effective heat capacity method was used for phase change modelling. The developed model was consequently coupled with the self-adaptive differential evolution optimization method. The cost function was defined as the root mean square error between the outlet SAC temperature and the set temperature. Using PCM parameters and its width as variables, the optimal set of parameters was determined. The optimal temperature of phase change was equal to 64.8 °C, PCM thickness 0.08 m and material parameter $c_1 = 69,997 \text{ J/kg} \cdot \text{K}$.

1. Introduction

Solar radiation plays a very important role in modern society since it is a clean and renewable source of energy. Solar radiation is utilized in solar thermal, solar photoelectric and solar chemical processes, where solar thermal process is the most common one (Li and Zhai, 2017). Solar energy, even if it is sometimes underestimated, can provide more than enough power to cover the world's energy demand (Ghiami and Ghiami, 2018). It has also other advantages compared to conventional systems such as availability and inexhaustibility. It also does not pollute the environment. However, solar energy still has some drawbacks. The mismatch between energy supply and demand could be significant and must be accounted for. This could be dealt with by integrating thermal energy storage (TES) into solar energy systems (Li and Zhai, 2017).

There are many different configurations in which solar air collectors could be developed, depending usually on the number of air flow channels and glazing. Most front-pass solar collectors are glazed, since glazing can significantly reduce heat losses into the surrounding environment (Charvát et al., 2019). In case of front and back pass collectors, there is a significant increase in the heat transfer surface area. Air flow in a front and back pass collector is in the same direction in both air channels, while in the case of a double pass collector, air flows in the opposite directions in each cavity.

Several studies on TES systems have been conducted in the last decade. One area where TES systems can be used are of solar air collectors, which have many different applications e.g. space heating (Enibe, 2003) or agricultural products withering (El Khadraoui et al., 2017). On the other hand, solar collectors are widely used for water heating purposes as a part of solar water heater (SWH) systems (Allouhi et al., 2018), which are a promising alternative for worldwide hot water supply. The study presented by (Allouhi et al., 2018) included design optimization, but just in terms of simple selection from several promising cases. PCMs are as well very useful for temperature fluctuation reduction. It has been shown that integrating PCMs into photovoltaic solar

modules may prolong their lifespan significantly (Grabo et al., 2019), however, at the cost of reducing generated electrical power. The experimental study conducted by (El Khadraoui et al., 2017) focused on the feasibility of the use of a solar air heater for nocturnal drying of crops. Two scenarios were investigated. The first one with PCM layer and the second without PCM. The PCM helped to maintain the night-time relative humidity between 17 % and 35 % lower, compared to the ambient relative humidity as well as drying chamber temperature between 4 - 16 °C. The experimental investigation was carried out by (Kabeel et al., 2016) dealing with flat and v-corrugated plate solar air heaters (SAH) with PCM used for TES purposes. The thermal performance parameters were studied for v-corrugated and flat-plate SAH both with and without PCM. The experimental results have shown that the v-corrugated SAH with PCM had daily efficiency 12 % higher in comparison with the one without PCM. It was as well 15 % higher compared to the flat plate SAH with PCM and 21.3 % higher compared to flat plate SAH without PCM. A solar crop dryer with TES was developed by (Jain and Tewari, 2015). The solar dryer had flat plate collector, packed bed TES system, drying chamber with crops and natural convection ventilation system. The temperature inside the drying chamber was 6 °C higher compared to ambient temperature from the sunshine hours and until midnight.

Most studies were focused primarily on numerical modelling and experimental methods with attention to numerical model validation and efficiency comparison between flat-plate/PCM solar air collectors. However, the suitable PCM and its parameters are usually determined considering only several promising scenarios (Allouhi et al. 2018). These scenarios are then compared and the best one, in terms of a given cost function, is chosen. This may provide reasonably accurate solutions in some cases, but due to the black-box behaviour of the most of complex numerical model, the cost function cannot be guaranteed to be convex and the optimal solution may not be possible to be estimated in this manner.

In the presented study, this behaviour is taken into account and black-box based optimization methods are employed as solvers, since they can effectively find an accurate solution, regardless of the convexity of the cost function or the feasible solution set. In order to make PCM SAC work efficiently under given conditions, the optimization study must be conducted as it leads to the reduction in energy consumption during agricultural products withering or space heating. Since PCM SACs are usually almost maintenance free, they could play an important role in terms of global carbon footprint reduction. Such devices could be easily used even in developing counties since they require almost little to none electrical power. In general, design and material optimization are able to provide higher efficiency of SAC or more stable outlet temperature, but the proposed methodology can be applied to any cost function related SACs. This study is focused on agricultural products withering. Solar air drying systems with TES are used to maintain continuity of the drying process, because of colour and flavour vulnerability of dried products. The main objective of this paper is the determination of the optimal design and material parameters of the front and back pass SAC for which the outlet air temperature is maintained at the desired value.

2. Methods

A front and back SAC with PCM-based solar absorber plate was considered in this study. The absorber plate consisted of 9 aluminium plates (usually referred to as compact storage modules (CSM) panels) which were filled with paraffin-based PCM. The frontal transparent cover of the SAC was made of plexiglass to reduce energy losses to the surroundings. The ambient air enters the SAC at the bottom part, and it is drawn through the air flow channels by axial fans which are located at the upper back side of the SAC. The opaque black paint with an absorbance of 0.9 was used to cover the CSM panels.

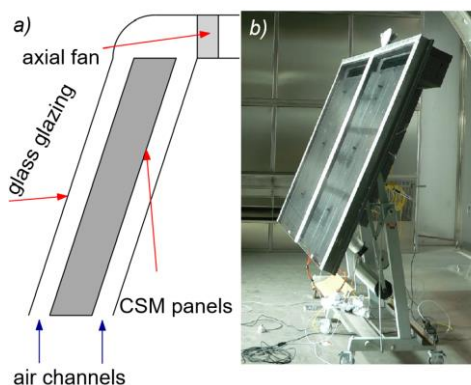


Figure 1: (a) A front and back pass SAC description; (b) experimental setup of front and back pass SAC used in (Charvát et al., 2019)

The dimensions of the solar absorber plate with PCM were $0.01 \times 0.9 \times 1.5$ m. Light-weight (LW) SAC was considered as well, in this case the absorber was made out of steel plate with dimensions of $0.0005 \times 0.9 \times 1.5$ m. The SAC description is shown in Figure 1a and the experimental setup in a climatic chamber with the solar simulator is in Figure 1b.

2.1 Numerical model

The governing equation in case of 2D heat conduction model is

$$\rho c_{\text{eff}} \frac{\partial T}{\partial \tau} = \frac{\partial}{\partial x} \left(k \frac{\partial T}{\partial x} \right) + \frac{\partial}{\partial y} \left(k \frac{\partial T}{\partial y} \right), \quad (1)$$

where T is temperature, τ is time, ρ is density, k is thermal conductivity, c_{eff} stands for effective heat capacity and x, y are spatial coordinates in PCM layer.

The effective heat capacity was defined in a form of Gaussian function as:

$$c_{\text{eff}} = c_0 + c_1 \exp \left\{ - \frac{(T - T_{\text{pch}})^2}{\sigma} \right\}, \quad (2)$$

where c_0 is heat capacity outside the phase change interval, c_1 is the highest value of heat capacity, T_{pch} is phase change temperature and σ defines the sharpness of given Gaussian function.

Heat conduction is solved using the energy balance approach coupled with control volumes method in its explicit form. This leads in case of 2D model to 9 explicit equations defining temperature in the $(p+1)$ -th time step using only temperatures from p -th time step.

$$T_{m,n}^{p+1} = f(T_{m,n}^p + T_{m+1,n}^p + T_{m-1,n}^p + T_{m,n+1}^p + T_{m,n-1}^p), \quad (3)$$

where $T_{m,n}^{p+1}$ is the temperature in $(p+1)$ -th time step and the temperature node with spatial coordinates m, n . Air flow is simulated using two 1D layers of air flowing around the solar absorber plate (CSM panels). The equations are derived in the same way in means of the energy balance and control volumes method and connected with PCM layer by Newton's cooling law as a boundary condition. The equations of air layers are based around basic energy balance, which can be written as:

$$T_{vz,n}^{p+1} = T_{vz,n}^p - \frac{\dot{Q}_{\text{conv}}}{\dot{m}c_{vz}} + \frac{\dot{Q}_{\text{loss}}}{\dot{m}c_{vz}}, \quad (4)$$

where $T_{vz,n}^{p+1}$ is the temperature of n -th air node, \dot{m} is mass flow rate and c_{vz} is the heat capacity of air. The amount of air nodes is determined by discretization in y -coordinate, which is equal to N_y . The convective heat flux is defined via Newton's cooling law as:

$$\dot{Q}_{\text{conv},n} = h L w (T_{vz,n}^p - T_{0,n}^p), \quad (5)$$

where h is the heat transfer coefficient, w is the size of the collector in z direction (width of CSM panel) and $L = \Delta y$, $\forall n \in (0, N_y)$ $L = \frac{\Delta y}{2}$, $n = 0, N_y$.

During every time step, the whole air gap layer is shifted up $T_{vz,n+1}^{p+1} = T_{vz,n}^{p+1}$, the $T_{vz,n}^{p+1}$ value is saved as air output temperature and the first value is replaced with current outside ambient temperature T_{amb} . Both ambient temperature T_{amb} and solar irradiance are measured during one characteristic summer day in Brno, Czech Republic. Acquired data are from permanent GPS station Technical University Brno (TUBO). The radiative heat flux is defined as:

$$\dot{Q}_{\text{rad}} = I(t) \Delta y w \tau \alpha_1, \quad (6)$$

where $I(t)$ is solar irradiance, τ is transmissivity of the glass cover and α_1 is absorptivity of the solar absorber plate (CSM panels). Similarly, the convective heat flux between non-irradiated air layer and back side of the PCM is defined as:

$$\dot{Q}_{\text{conv}1,n} = h L w (T_{vz1,n}^p - T_{N_x,n}^p). \quad (7)$$

PCM, considered as a thermal storage material inside the solar absorber plate was supposed to have the properties of paraffin-based Rubitherm RT series. Considering manufacturers data and the effective heat capacity method, it corresponds to $c_0 = 2,000$ J/kg·K, $c_1 = 61,300$ J/kg·K, $T_{\text{pch}} = 41$ °C and $\sigma = 2.1$ K² in case of Rubitherm RT 42. This material is taken as a blueprint during the optimization study where T_{pch} and c_1

parameters are used as variables. A sunny summer day in Brno, Czech Republic was chosen and input parameters such as solar irradiance $I(t)$ and ambient temperature $T_{\text{amb}}(t)$ are shown in Figure 2.

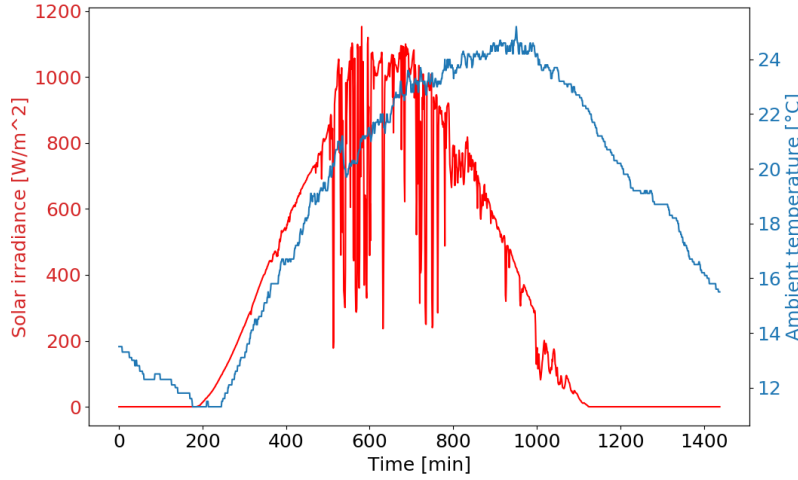


Figure 2: The solar irradiance and ambient temperature 17/7/2019 in Brno, Czech Republic

The thickness d of the solar absorber plate (CSM panel), parameter c_1 from the effective heat capacity curve defined by Eq(2) and the phase change temperature T_{pch} were chosen as the optimization parameters. The bounds were set as $d \in [0.001; 0.1]$ m, $c_1 \in [30,000; 70,000]$ J/kg · K and $T_{\text{pch}} \in [35; 75]$ °C. The initial conditions for both air layers and PCM layer are equal to ambient temperature at time 0 s – $T_{\text{amb}}(0)$.

The cost function is defined as a root square mean error (RMSE) between output temperature from simulation T_{vz, N_y} and the set temperature T_{set} which is the desired temperature at the SAC outlet. Set temperature was chosen as $T_{\text{set}} = 40$ °C. The goal of this optimization task is to find optimal parameters for which outlet temperature will be as close as possible to the set temperature. The cost function is defined as:

$$f(d, c_1, T_{\text{pch}}) = \sum_{\rho=0}^{t_{\text{max}}} \left(T_{vz, N_y}^{\rho+1} - T_{\text{set}} \right)^2. \quad (8)$$

3. Results

The numerical model of the SAC was validated with the use of experimental data obtained in the climatic chamber investigation (Charvát et al., 2019). There is a good agreement between the numerical model of the SAC and the experimental data, besides some discrepancies which may be caused by model simplification. Heat losses from the air layer are neglected and some parameters such as the air flow rate, air density etc. are considered constant in time. There is an observable difference in the ramping-up part during the first hour of simulation, which may be caused by not accounting for the whole mass of the solar air collector and working just with the mass of PCM layer. The numerical model is capable of capturing the behaviour well enough, considering that the main focus of this study is proof of the concept of the optimization part. Results of the validation are shown in Figure 3.

3.1 Optimization

The self-adaptive differential evolution (sa-DE) was used during optimization. The optimal solution was determined as $d = 0.08$ m, $c_1 = 69,997$ J/kg · K and $T_{\text{pch}} = 64.8$ °C. A reference case in the optimization study was a light-weight SAC with the solar absorber plate made of metal sheet of the thickness $d = 0.5$ mm with thermal conductivity $\lambda_{\text{lw}} = 40$ W/m · K and heat capacity $c_{\text{lw}} = 460$ J/kg · K.

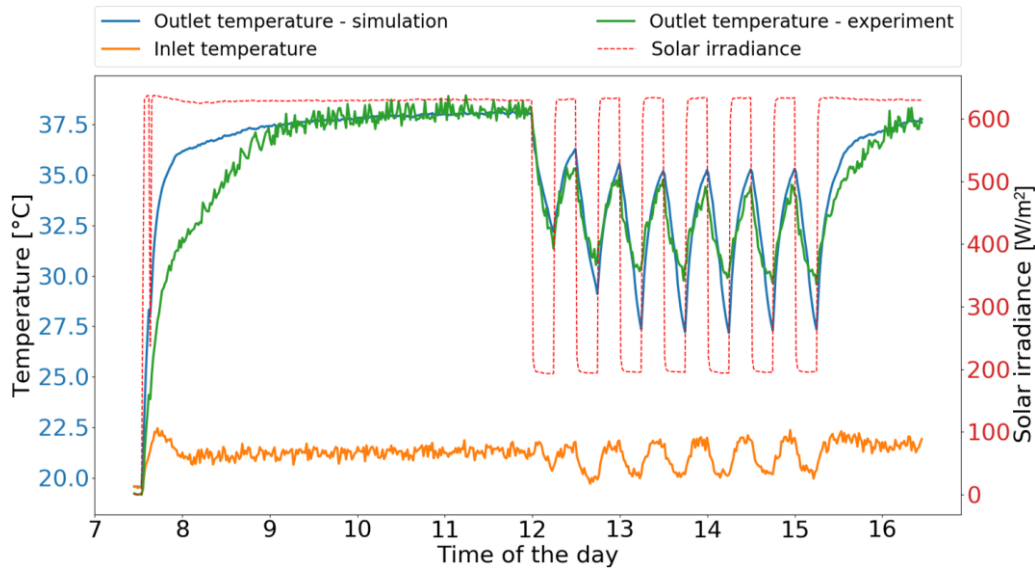


Figure 3: Validation of the numerical model – comparison between simulation and experiment

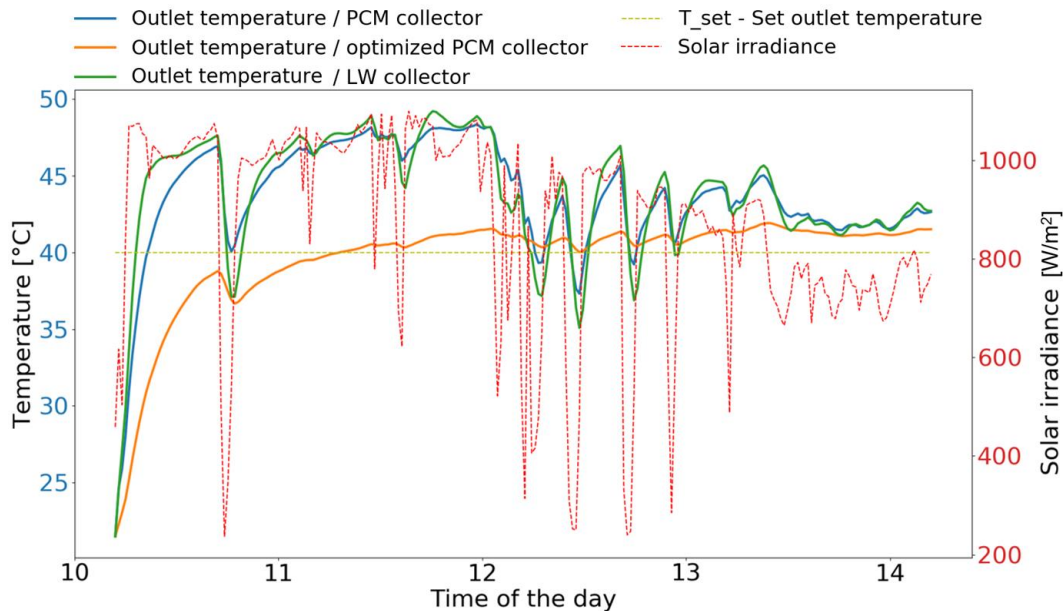


Figure 4: Comparison between outlet temperatures of the optimized PCM SAC, PCM SAC with $d = 0.01$ m and LW SAC

The corresponding outlet temperature is shown in Figure 4. There are two other scenarios used for comparison with the optimized PCM collector. The first one is the reference LW SAC. The second is the PCM SAC with the solar absorber thickness $d = 0.01$ m and other parameters same as in the optimized scenario. There is a significant improvement in the outlet air temperature stability in case of the optimized PCM collector compared to both the LW and thin PCM collector. The temperature stabilization was quantified in terms of the temperature range reduction in the time interval from 11:00 to 14:00. The outlet temperature in case of the LW SAC was between 35.1 - 49.2 °C. The thin PCM absorber plate was able to stabilize outlet temperature to 37.3 - 48.3 °C and the optimized PCM SAC reduced the outlet air temperature fluctuations to 39.7 - 41.9 °C, so there is a considerable improvement with the increase of the PCM thickness. However, the cost function should be penalized for the amount of PCM in CSM panels, because 0.08 m is rather unusual thickness and material costs would be much higher.

4. Conclusion

The results of the optimization study have shown that a solar air collector with PCM in the solar absorber plate can provide more stable outlet air temperature than a lightweight solar air collector. The study was conducted for a sunny summer day in the Czech Republic and more scenarios need to be investigated in the future to explore the effectiveness of this concept under different climatic and operating conditions.

The main outcomes of the present study:

- PCM-based thermal energy storage integrated with the solar absorber plate has the potential to stabilize the outlet air temperature of solar air collectors under varying boundary conditions.
- Self-adaptive differential evolution algorithm was effectively used in the search for the optimal thickness of the PCM layer in the solar absorber plate.
- The outlet air temperature fluctuations were reduced from 35.1 - 49.2 °C in case of the lightweight solar air collector to 39.7 - 41.9 °C in case of the collector with the optimised thickness of the PCM layer.
- The objective function should include not only thermal performance parameters but also parameters (and their feasible ranges) reflecting the techno-economic constraints of the solar air collector design. The future work will focus on these issues.

Acknowledgements

This work was supported by the Czech Science Foundation under the contract 18-19617S "Hysteresis of the temperature-enthalpy curve during partial phase change of latent heat storage materials." and by the project "Sustainable Process Integration Laboratory – SPIL", No. CZ.02.1.01/0.0/0.0/15_003/0000456, funded by European Research Development Fund, Czech Republic Operational Programme Research, Development and Education, Priority 1: Strengthening capacity for quality research.

References

- Allouhi A., Ait Msaad A., Benzakour Amine M., Saidur R., Mahdaoui M., Kousksou T., Pandey A. K., Jamil A., Moujibi N., Benbassou A., 2018, Optimization of melting and solidification processes of pcm: application to integrated collector storage solar water heaters (ICSSWH), *Solar Energy*, 171, 562–570.
- Charvát P., Klímeš L., Pech O., Hejčík J., 2019, Solar air collector with the solar absorber plate containing a PCM – environmental chamber experiments and computer simulations, *Renewable Energy*, 143, 731-74.
- El Khadraoui, A., Bouadila S., Kooli S., Farhat A., Guizani A., 2017, Thermal behavior of indirect solar dryer: nocturnal usage of solar air collector with PCM, *Journal of Cleaner Production*, 148, 37–48.
- Enibe S. O., 2003, Thermal analysis of a natural circulation solar air heater with phase change material energy storage, *Renewable Energy*, 28, 2269 - 2299.
- Ghiami A., Ghiami S., 2018, Comparative study based on energy and exergy analyses of a baffled solar air heater with latent storage collector, *Applied Thermal Engineering*, 133, 797–808.
- Grabo M., Weber D., Paul A., Klaus T., Bempohl W., Krauter S., Kenig E.Y., 2019, Numerical investigation of the temperature distribution in PCM-Integrated solar modules, *Chemical Engineering Transactions*, 76, 895–900.
- Jain D., Tewari P., 2015, Performance of indirect through pass natural convective solar crop dryer with phase change thermal energy storage, *Renewable Energy*, 80, 244–250.
- Kabeel A. E., Khalil A., Shalaby S. M., Zayed M. E., 2016, Experimental investigation of thermal performance of flat and V-corrugated plate solar air heaters with and without PCM as thermal energy storage, *Energy Conversion and Management*, 113, 264–272.
- Li B., Zhai X., 2017, Experimental investigation and theoretical analysis on a mid-temperature solar collector/storage system with composite PCM, *Applied Thermal Engineering*, 124, 34–43.